

1 **Responses of soil respiration to rainfall pulses in a natural grassland**
2 **community on the semi-arid Loess Plateau of China**

3
4 Furong Niu^{a,c,#}, Ji Chen^{a,c}, Peifeng Xiong^a, Zhi Wang^{a,b}, He Zhang^a, Bingcheng Xu^{a,b,*}

5
6 ^a *State Key Laboratory of Soil Erosion and Dryland Farming on the Loess Plateau, Northwest A&F*
7 *University, Yangling, Shaanxi Province 712100, China*

8 ^b *Institute of Soil and Water Conservation, Chinese Academy of Sciences and Ministry of Water Resources,*
9 *Yangling, Shaanxi Province 712100, China*

10 ^c The two authors are equal contributors.

11
12 # Current address: School of Natural Resources and the Environment, University of Arizona, Tucson, AZ,
13 85721, USA

14 * Corresponding author

15 Dr. Bingcheng Xu. State Key Laboratory of Soil Erosion and Dryland Farming on the Loess Plateau,
16 Northwest A&F University, Yangling, Shaanxi Province, 712100, China.

17 E-mail: Bcxu@ms.iswc.ac.cn

19 **Abstract**

20 Pulsed rainfall affects both aboveground vegetation dynamics and belowground biogeochemical
21 processes, such as carbon cycling, in semi-arid regions. In order to study carbon released by soil respiration
22 (SR) after rainfall pulses in natural grassland on the Loess Plateau, a rainfall simulation experiment was
23 conducted in a grassland community co-dominated by a C₄ herbaceous grass [*Bothriochloa ischaemum* (L.)
24 Keng] and a C₃ leguminous subshrub [*Lespedeza davurica* (Laxm.) Schindl] in the loess hilly-gully region.
25 Soil respiration rate (R_s), soil temperature (T_s), and soil volumetric water content (S_v) were measured 1 day
26 before and 1, 2, 3, 5, and 7 days after four rainfall treatments (ambient rainfall plus a 5 mm, 10 mm, 20 mm,
27 and 30 mm rainfall pulse) and one control treatment (only ambient rainfall) in June and August 2013.
28 Results showed that R_s and S_v largely increased one day after simulated rainfall greater than 5 mm. In June,
29 the peak R_s under 10, 20, and 30 mm rainfall was 0.80–1.03 $\mu\text{mol C m}^{-2} \text{s}^{-1}$ in *B. ischaemum*, with a 25–62%
30 increase compared with the control treatment, and 0.74–1.0 $\mu\text{mol C m}^{-2} \text{s}^{-1}$ (+51–104%) in *L. davurica*. In
31 August, the peak R_s was 1.23–1.73 $\mu\text{mol C m}^{-2} \text{s}^{-1}$ (+23–73%) and 1.52–1.70 $\mu\text{mol C m}^{-2} \text{s}^{-1}$ (+81–102%)
32 in *B. ischaemum* and *L. davurica*, respectively. The magnitude and duration of the increase in SR were
33 positively related to the rainfall size, and a more considerable increase was observed in August. There was
34 a threshold rainfall (i.e., 5–10 mm) for triggering SR increases in both months. And different responses
35 were found between the two species, there was more substantial SR increases in *L. davurica* in comparison
36 to *B. ischaemum*. After rainfall pulses, soil moisture and soil temperature co-regulated SR. During the
37 relatively dry season (i.e., June), SR was negatively correlated with soil temperature and the temperature
38 sensitivity Q_{10} value of SR was small (0.5–0.6), while it changed to positively in August and the Q_{10} was
39 largely increased (3.2–4.3). Conversely, soil moisture was positively related to SR in both months and
40 explained a large portion of the variation in SR (32–43% and 42–52% in *B. ischaemum* and *L. davurica*,

41 respectively). These findings indicated that soil moisture was the major environmental factor in controlling
42 SR in this grassland. Overall, our study suggests that SR response following rainfall pulses is
43 species-specific within the grassland community and tends to be controlled by soil moisture, and these
44 should be considered in the regional carbon budget assessment in the background of vegetation
45 rehabilitation and rainfall pattern changes.

46

47 **Keywords:** climate change; Q_{10} value; semi-arid grassland; simulated rainfall; soil CO₂ efflux

48

49 **Abbreviations**

50 Soil respiration (SR)

51 Soil respiration rate (R_s),

52 Soil temperature (T_s),

53 Soil volumetric water content (S_v)

54 Loess Plateau (LP)

55 Temperature sensitivity value of soil respiration (Q_{10})

56 **1. Introduction**

57 Soil respiration (SR), the process of CO₂ being released through respiration by heterotrophs (e.g., soil
58 microbes) and autotrophs (e.g., plant roots) in the soil, is a key component in the global carbon cycle and
59 the second largest carbon efflux in terrestrial ecosystems (Schlesinger and Andrews, 2000). A small change
60 in SR will notably influence the atmospheric CO₂ concentration and eventually affect the climate
61 (Schlesinger and Andrews, 2000). Spatio-temporally, SR is controlled by various biotic and abiotic factors,
62 and among those, soil temperature and soil moisture are two principal environmental drivers (Chen et al.,
63 2010; Davidson et al., 1998; Fóti et al., 2016; Xu et al., 2004). The dependence of SR on soil temperature is
64 commonly found when soil moisture is not limited (Fang and Moncrieff, 2001; Lloyd and Taylor, 1994).
65 When this occurs, an increase in temperature could improve the metabolism of soil microbes and plant
66 roots, subsequently increasing SR. On the other hand, SR could be decoupled with soil temperature and
67 even decreased with increasing temperature under drought or extreme wet conditions; in these
68 circumstances, soil moisture tends to be the main determinant of SR (Almagro et al., 2009; Chang et al.,
69 2014; Wang et al., 2014; Li et al., 2008). In water-limited semi-arid regions, rainfall pulses could result in
70 dry-wet cycles which could alter the soil micrometeorology (e.g., soil moisture and soil temperature), and
71 consequently affect the soil CO₂ efflux, increasing its instability, and adding uncertainty for assessing the
72 regional carbon budget.

73 The arid and semi-arid ecosystems dominantly determine the inter-annual variability and the changing
74 trend of global carbon sequestration (Ahlström et al., 2015). In such water-limited areas, discrete and
75 episodic pulsed rainfall is the major water input and it controls most aspects of ecosystem structure and
76 function (Noy-Meir, 1973), including aboveground biological processes (e.g., plant growth) (Schwinning
77 and Sala, 2004) and belowground biogeochemistry (e.g., carbon and nutrient cycling) (Austin et al., 2004).

78 The increase of SR following rainfall, which is termed as “Birch effect” (Birch 1958), has been widely
79 reported across different ecosystems (see reviews by Boriken and Matzner, 2009; Kim et al., 2012). In arid
80 and semi-arid regions, significant and prompt increases of SR following rainfall pulses has been
81 extensively reported in desert grasslands/shrublands (Sponseller, 2007; Cable et al., 2008; Thomey et al.,
82 2011), semi-arid grasslands (Chen et al., 2008; López-Ballesteros et al., 2016; Wei et al., 2016), and
83 Mediterranean forests (Almagro et al., 2009; Unger et al., 2010). Their results suggest that besides soil
84 temperature and soil moisture, other biotic and abiotic factors also co-regulate the SR response after pulsed
85 rainfall. Firstly, the aboveground vegetation affects the soil microenvironment and influences soil CO₂
86 efflux via root respiration (Raich and Tufekciogul, 2000). Secondly, the soil properties such as soil texture,
87 soil organic matter, and antecedent soil water content could regulate the SR fluctuation following rainfall.
88 Cable et al. (2008) found that fine-textured soils could release more CO₂ following a pulse event, and
89 Harrison-Kirk et al. (2013) reported that soil with more organic matter had larger SR increments, while the
90 antecedent soil water content has been widely found to be negatively correlated with the SR responses after
91 rainfall (Cable et al., 2008; Liu et al., 2017; Xu et al., 2004). Lastly, rainfall characteristics as could be
92 expected, especially the magnitude and timing of pulse events greatly affect SR, and large rainfall pulses
93 may result in more substantial SR increases than small ones, and timing could determine antecedent soil
94 water content and other soil microenvironments (Cable et al., 2008; Schwinning and Sala, 2004; Song et al.,
95 2012; Thomey et al., 2011).

96 The Loess Plateau (LP), located in the upper-middle reach of the Yellow River in northern China, is
97 well-known for its severe soil and water erosion, sparse vegetation, and dry environment. Over the past
98 decades, its vegetation coverage increased largely after implementation of the “Grain for Green” project
99 which focuses on returning over-cultivated croplands to natural forest/grassland (Li et al., 2017). Currently,

100 the natural grassland is the most widely distributed vegetation type in the region, which accounts for about
101 42% of the total land area of LP (Li et al., 2016). Long-term climate data suggests that annual precipitation
102 across the whole LP region may remain unchanged, but the intra-annual variability increased with more
103 extreme precipitation events and longer drought duration during 1961–2011 (Miao et al., 2016; Peng et al.,
104 2017). The extensive vegetation restoration accompanied by precipitation regimes changes will
105 undoubtedly alter the SR process in the local natural grassland. Therefore, clarifying responses of SR to
106 pulsed rainfall in this widely distributed vegetation is significant for projecting the regional carbon budget.

107 *Bothriochloa ischaemum* (L.) (a C₄ perennial herbaceous grass) and *Lespedeza davurica* (Laxm.)
108 Schindl. (a C₃ perennial leguminous subshrub), are the two native and dominant species in the local natural
109 grassland community, and both have important ecosystem functions in reducing soil and water erosion (Xu
110 et al., 2011). Previous studies found that the two species responded significantly and positively with
111 photosynthesis to simulated rainfall pulses, and *B. ischaemum* was more sensitive to small rainfall pulses
112 (5–10 mm) than *L. davurica* (Niu et al., 2016; Xiong et al., 2017). These species-specific responses in
113 carbon assimilation after rainfall may alter the community composition and structure in the long run (Niu et
114 al., 2016). On the other hand, as the primary cause of carbon loss, the SR response to rainfall pulses
115 remains unknown in this natural grassland community. Furthermore, plant functional traits (e.g., grass vs.
116 legume) could influence SR (De Deyn et al., 2008), which adds uncertainty for evaluating soil carbon
117 efflux at the community level in the background of an altered vegetation community. Thus, to investigate
118 the effects of rainfall pulses on SR in such a semi-arid ecosystem and understanding SR response in the
119 species-level, a simulated rainfall experiment was conducted in the two species co-dominated natural
120 grassland community, and the SR fluctuations after rainfall were monitored. The objectives were: 1) to
121 clarify the SR changes after rainfall events with different sizes and occurred in different growing periods, 2)

122 to compare the response differences between the two dominant species, and 3) to distinguish the
123 dependence of SR on soil temperature and soil moisture after pulsed rainfall.

124 **2. Materials and methods**

125 *2.1. Site description*

126 The study was conducted at the Ansai Research Station of Soil and Water Conservation, Chinese
127 Academy of Sciences (109°19'23" E, 36°51'31" N), Shaanxi Province, China. The climate in the region is
128 characterized as temperate mid-continental. The annual average temperature is 8.8 °C, with the lowest
129 mean temperature of -6.9 °C in January and the highest mean temperature of 22.6 °C in July. Average
130 annual rainfall is around 540 mm (1951–2000), with more than 60% occurring from July to September,
131 which is typically the rainy season. The silty loam soil was developed from wind deposits and is classified
132 as Calcaric Cambisol (Zhang et al., 2011). The semi-arid meadow-steppe is the most distributed vegetation
133 type and accounts for ~42% of the total land area in the region (Li et al., 2016).

134 The investigated grassland community is homogeneously distributed in a mountain slope (109°19'07" E,
135 36°51'15" N; 1150 m a.s.l.), with slope degree of 24° and slope aspect SE10°. The *B. ischaemum* and *L.*
136 *davurica* are co-dominant species in the community, and other main species include *Stipa bungeana* Trin.,
137 *Artemisia sacrorum* Ledeb., *Artemisia vestita* Wall. ex Bess., and *Astragalus melilotoides* Pall. The
138 community vegetation coverage was $57 \pm 2\%$ and $80 \pm 1\%$ in June and August 2013, respectively. The
139 species coverage of *B. ischaemum* and *L. davurica* was $35 \pm 4\%$ and $46 \pm 4\%$ in June, $35 \pm 3\%$ and $34 \pm 3\%$
140 in August 2013, respectively.

141 *2.2. Rainfall simulation*

142 Rainfall simulation was carried out using a homemade portable rainfall simulator (Chinese patent, No.
143 ZL2013103763306), and details can be found in Xiong et al. (2017). The sprinklers of the simulator are

144 about 2.0 m above the grassland canopy, and the rainfall intensity was set at 0.5 mm/min, which resembles
145 the characteristics of the local rainfall event (Zhang et al., 2017). The rainfall simulation was conducted on
146 June 12th (relatively dry period and the beginning of the growing season) and August 15th (the rainy season
147 and middle of the growing season) in 2013. Two study blocks were established in the homogenous
148 grassland community, the block one was randomly chosen for the experiment in June, and the block two
149 was for the experiment in August (see Fig. 1).

150 According to long-term precipitation data in 2005–2013, the local natural rainfalls were mainly small
151 and medium events (i.e., 0–10 mm and 10–25 mm), infrequently accompanied by large and extreme events
152 (i.e., 30 mm and above 50 mm) (Zhang et al., 2017). Thus, four different simulated rainfall treatments were
153 set up as ambient rainfall plus single rainfall pulses at 5 and 10 mm (small rainfall), 20 mm (medium
154 rainfall), and 30 mm (large rainfall), and a control treatment only receiving the ambient. Each treatment
155 was randomly applied to a plot within one specific block, with three replicates per treatment (i.e., rainfall
156 size; Fig. 1). The plot size was 1.0 m by 1.0 m with 1.0 m space between neighboring plots to avoid
157 potential influences. The rainfall simulation was conducted in the early morning or late afternoon to reduce
158 potential water loss due to evaporation.

159 2.3. Soil respiration measurement

160 The two dominant species (i.e., *B. ischaemum* and *L. davurica*) account for at least 50% of the total
161 vegetation coverage in the studied grassland community throughout the whole growing season (Duan et al.
162 unpublished data). Therefore, their soil respiration could well represent a large proportion of the
163 community total and were selected for soil respiration measurement in this study. In each plot, one bunch of
164 *B. ischaemum* and one single *L. davurica* plant were randomly selected for the measurement. All their
165 aboveground biomass including living and dead parts were completely clipped and removed two days

166 before the rainfall simulation to exclude the respiration from aboveground plant materials. The soil
167 respiration rate (R_s ; $\mu\text{mol C m}^{-2} \text{ s}^{-1}$) was measured between 9:00–11:00 a.m. on 1 day before and 1, 2, 3, 5,
168 and 7 days after simulated rainfalls during each experimental period by using an enclosed-chamber CO_2
169 efflux measurement system (EGM-4 IRGA connected to an SRC-1 soil respiration chamber; PP-Systems,
170 Amesbury, MA, USA). For each measurement, the CO_2 concentration was recorded for 30s at 4s intervals.

171 *2.4. Environmental factors*

172 Annual rainfall data in 2013 was obtained from a meteorological station near the study site (ca. 500 m).
173 Soil volumetric water content (hereafter referred to as “soil water content”; S_v , %; 0–20 cm) was measured
174 using a neutron moisture meter (CNC503B, Sper Energy, Nuclear Technology Ltd., Beijing, China) in the
175 center of each plot. Soil temperature (T_s ; $^{\circ}\text{C}$) was measured at a 10 cm depth using digital thermometers
176 (TP101, Xinhua Junhui Electric Appliances Factory, Jiangsu Province, China) for the soils below the
177 studied grasses and shrubs. All measurements were performed on 1 day before and 1, 2, 3, 5, and 7 days
178 after rainfall treatments and simultaneously with soil respiration measurements. Average air temperature
179 (T_a ; $^{\circ}\text{C}$) between 9:00–11:00 a.m. on each day was obtained from a portable photosynthesis system
180 (CIRAS-2; PP SYSTEMS, Haverhill, MA, USA), which was used for parallel gas exchange measurements
181 in the same plots (Shu, 2014).

182 *2.5. Statistical analysis*

183 The effects of measurement month, species, and rainfall size, and their interactions on soil water
184 content (S_v), soil temperature (T_s), and soil respiration rate (R_s) were analyzed by two-way/three-way
185 ANOVA. The S_v , T_s , and the peak R_s values under different rainfall treatments were tested by one-way
186 ANOVA with the Tukey post-hoc test ($P \leq 0.05$). All data were checked for normality (Shapiro-Wilk test)
187 and homogeneity of variances (Levene’s test) prior to ANOVA. The Mann-Whitney test was used to

188 compare unpaired data in case their normality could not be obtained through data transformation. The
189 relationship between R_s and T_s after simulated rainfall was studied using the exponential function (van't
190 Hoff 1898):

$$191 \quad R_s = a \times e^{bT_s} \quad (1)$$

192 Where a and b are fitted parameters. R_s and T_s are soil respiration rate and soil temperature of the two
193 species measured on different days after rainfall. The temperature dependence of soil respiration on soil
194 temperature is commonly expressed by Q_{10} value, which is derived by:

$$195 \quad Q_{10} = \exp^{10 \times a} \quad (2)$$

196 Where a is the parameter obtained from the equation (1). The relationships between R_s and S_v or combining
197 T_s and S_v were studied using the logarithmic (equation 3) and binary linear functions (equation 4) following
198 Chen et al. (2008):

$$199 \quad R_s = a \times \ln S_v + b \quad (3)$$

$$200 \quad R_s = a \times S_v + b \times T_s + c \quad (4)$$

201 Where a , b , and c are fitted parameters. R_s and S_v are soil respiration rate and soil water content measured
202 on different days after rainfall treatments. All statistical tests were performed with SPSS 17.0 (SPSS Inc.,
203 Chicago, IL, USA).

204

205 **3. Results**

206 *3.1. Natural rainfall in 2013*

207 The annual rainfall was 725 mm in the study site in 2013, which was 36% higher than the long-term
208 average (532 mm; 1951–2010). The rainfall amount during the growing season (April–October) was 709
209 mm, 44% higher than the long-term mean (493 mm) (Fig. 2). Before rainfall simulation in June, there were

210 no rainfalls bigger than 5 mm, except a 13.4 mm event on April 19th, and the monthly rainfall amount in
211 June was 66 mm. The summed rainfall amount was 590 mm during the rainy season (July–September),
212 which accounts for 81% of the yearly total. An extremely high monthly amount (417 mm) was observed in
213 July, which is about 3.5 times of the long-term average (118 mm). No natural rainfall events occurred three
214 days before or seven days after the rainfall simulation during the two experimental periods.

215 3.2. Soil water content (S_v), air temperature (T_a), and soil temperature (T_s)

216 Both experimental month and rainfall treatment significantly affected S_v ($P < 0.001$; Table 1). In
217 general, S_v in August was about 6.0%, which was 22% higher than in June (average 4.9%) across all
218 rainfall treatments (Fig. 3). Under the control treatment, S_v remained stable (ca. 4.5%) during the
219 experimental period in June, while in August it decreased gradually (ranged from 5.2–6.4%; Fig. 3). In both
220 months, S_v under 5 mm rainfall showed similar changing trends as the control, and there was no substantial
221 difference between values under these two ($P > 0.05$; Fig. 3). Under 10 mm, 20 mm, and 30 mm rainfall
222 treatments, S_v increased (+16–38%) with respect to the control on the first day after rainfall and then
223 decreased (Fig. 3). In June, S_v values under 10 mm, 20 mm, and 30 mm rainfall treatments were
224 significantly higher than under the control and 5 mm treatments from the first to the third day after rainfalls
225 ($P < 0.05$). On the fifth day, there were no differences among all treatments (Mann-Whitney test, $P > 0.05$).
226 The maximum S_v value (6.1%) was observed under 30 mm treatment on the first day after rainfall, which
227 was 38% higher than the control on the same day (Fig. 3). In August, S_v values largely increased under 10
228 mm, 20 mm, and 30 mm treatments (+8%, +7%, and +23%) compared with the control one day after
229 rainfall, while there were no significant differences in S_v between rainfall treatments and the control ($P >$
230 0.05; Fig. 3).

231 Air temperature (T_a) fluctuated during the two experimental periods, and the average value was around

232 30 °C in both months (Fig. 4). The soil temperature (T_s) showed similar changing trends between the two
233 species ($P > 0.05$; Fig. 4 and Table 1), but varied significantly in the two months ($P < 0.001$; Table 1). In
234 June, compared with the control, T_s only decreased on the first day after rainfall in *B. ischaemum*, and
235 decreased by 4%, 15%, 7%, and 14% under 5 mm, 10 mm, 20 mm, and 30 mm treatments, respectively,
236 and the values ranged from 16.9–18.5 °C (Fig. 4). However, in *L. davurica*, T_s decreased by a comparable
237 extent (3–9%; ranging from 17.5–17.8 °C) under all (including control) treatments one day after rainfall
238 simulation (Fig. 4). From the second to the seventh day, T_s increased gradually and closely followed the
239 change of T_a in both species. In August, in comparing with the control, T_s slightly decreased on the first day
240 after each rainfall treatment in both species, and the values were 25.7 ± 0.2 °C and 25.8 ± 0.3 °C for *B.*
241 *ischaemum* and *L. davurica*, respectively. From the second day after simulated rainfalls, T_s started to mirror
242 the fluctuation of T_a in both species (Fig. 4).

243 3.3. Soil respiration rate (R_s)

244 The experimental month, rainfall size, species, and interaction of species with rainfall size had
245 significant effects on R_s (Table 1). In June, the 5 mm rainfall did not considerably affect the R_s in both
246 species (Fig. 5). Under 10 mm, 20 mm, and 30 mm rainfall treatments, R_s largely increased compared with
247 the control treatment on the first day, while it started to decrease and remained relatively stable towards the
248 seventh day, and the values under rainfall treatments were higher than the control treatment until the
249 seventh day in *B. ischaemum* and the fifth day in *L. davurica* (Fig. 5). During the whole experimental
250 period, the peak R_s values under 10 mm, 20 mm, and 30 mm treatments were 0.80 ± 0.27 $\mu\text{mol C m}^{-2} \text{s}^{-1}$,
251 1.03 ± 0.13 $\mu\text{mol C m}^{-2} \text{s}^{-1}$, and 0.97 ± 0.07 $\mu\text{mol C m}^{-2} \text{s}^{-1}$ in *B. ischaemum*, which were appeared on the
252 first day after rainfall, and were 25%, 62%, and 53% higher than the control treatment, respectively, but
253 their differences were not significant ($P > 0.05$; Fig. 6). In *L. davurica*, the maximum values of R_s also

254 appeared on the first day after simulated rainfalls, and were $0.74 \pm 0.03 \mu\text{mol C m}^{-2} \text{ s}^{-1}$, $0.85 \pm 0.01 \mu\text{mol}$
255 $\text{C m}^{-2} \text{ s}^{-1}$, and $1.00 \pm 0.02 \mu\text{mol C m}^{-2} \text{ s}^{-1}$ for 10 mm, 20 mm, and 30 mm treatments, respectively, which
256 were all significantly higher than the control (+51%, +74%, and +104%) ($P < 0.05$; Fig. 6).

257 In August, R_s drastically increased on the first day after simulated rainfall in both species, except under
258 5 mm treatment in *L. davurica*, then decreased sharply since the second day and remained relatively stable
259 thereafter (Fig. 5). The peak R_s values occurred on the first day after simulated rainfall, and were $1.23 \pm$
260 $0.09 \mu\text{mol C m}^{-2} \text{ s}^{-1}$, $1.66 \pm 0.09 \mu\text{mol C m}^{-2} \text{ s}^{-1}$, and $1.73 \pm 0.10 \mu\text{mol C m}^{-2} \text{ s}^{-1}$ under 10 mm, 20 mm, and
261 30 mm treatments in *B. ischaemum*, about 23%, 66%, and 73% higher than control, respectively. They
262 were only significantly higher than the control under the 20 mm and 30 mm rainfall treatments ($P < 0.05$;
263 Fig. 6). Likewise, the peak R_s values in *L. davurica* were also observed on the first day after simulated
264 rainfalls, which were $1.52 \pm 0.05 \mu\text{mol C m}^{-2} \text{ s}^{-1}$, $1.59 \pm 0.19 \mu\text{mol C m}^{-2} \text{ s}^{-1}$, and $1.70 \pm 0.09 \mu\text{mol C m}^{-2}$
265 s^{-1} under 10 mm, 20 mm, and 30 mm treatments, about 81%, 89%, and 102% higher than control,
266 respectively (Fig. 6).

267 3.4. Relationships of R_s with T_s and S_v

268 In June, R_s was negatively correlated with T_s in both *B. ischaemum* and *L. davurica* and could explain
269 10% and 25% of the variation of R_s , respectively (Figs. 7 and 8). While in August, R_s was positively
270 correlated with T_s and explained 24% and 22% of the variation, respectively (Figs. 7 and 8). The Q_{10} values
271 were 0.61 and 0.45 for *B. ischaemum* and *L. davurica* in June and increased to 3.22 for *B. ischaemum* and
272 4.31 for *L. davurica* in August, respectively (Table 2). The R_s was positively correlated with S_v in both
273 species and months (Figs. 7 and 8), and S_v could explain 32–52% of the variation in soil respiration with
274 the logarithmic functions. Using the binary linear function, T_s and S_v together could explain 33% and 47%
275 of the variation in soil respiration in *B. ischaemum* and *L. davurica* in June, and 56% and 60% of the

276 variation in August, respectively (Table 2).

277

278 4. Discussion

279 A significant increase in S_v and R_s was observed on the first day after rainfall pulses, then gradually
280 decreased and had no significant difference with the control treatment on the 5th–7th day after rainfall in
281 both species during the two experimental months (Figs. 3 and 5). Drastic but different degrees of increase
282 in soil CO₂ efflux following rainfall/watering has been well documented in many water-limited ecosystems,
283 e.g., in Inner Mongolian Steppe (Chen et al., 2008; Li et al., 2018), semi-arid grasslands in North America
284 and Mediterranean regions (López-Ballesteros et al., 2016; Thomey et al., 2011), and also grassland on the
285 Loess Plateau region (Jia et al., 2014). In this study, the burst of SR was recorded on the first day after
286 rainfall pulses, which is consistent with the ‘Birch effect’ (Birch 1958) and results from other
287 above-mentioned semi-arid grasslands (e.g., Chen et al., 2008; López-Ballesteros et al., 2016). While the
288 degree of increase was lower in this study (up to 73% and 102% in *B. ischaemum* and *L. davurica*,
289 respectively) comparing with others, such as an 8-times increase in Inner Mongolian Steppe (Chen et al.,
290 2008). The difference is likely due to the fact that other studies applied much larger rainfall pulses than this
291 study (e.g., 100 mm vs. maximum 30 mm), the larger rainfall could generally trigger more significant
292 ecosystem responses (Schwinning and Sala, 2004). A study in grassland in SE Spain also observed an up to
293 8–10 times increase immediately after receiving a rainfall pulse close to our study (i.e., 15 mm), but it
294 decreased to 2–3 times one day after watering (López-Ballesteros et al., 2016), which is similar to what we
295 observed and this could also indicate the effect of rainfall pulses declines over time. Increased soil
296 respiration following pulsed rainfall observed in this and other studies could be broadly attributed to
297 mechanisms like enhanced soil microbial metabolism by more substrate supply through decomposition of

298 dead microorganisms/fine roots/mycorrhiza and mineralization of physical protected soil organic matter
299 caused by changes of soil aggregate in dry-wet processes, and physical processes like water displacing CO₂
300 accumulated in soil pores by infiltration (Borken and Matzner, 2009; Chen et al., 2008; Kim et al., 2012;
301 Unger et al., 2010).

302 The size and timing of rainfall pulses control the magnitude and duration of SR response in many
303 semi-arid grassland communities (Chen et al., 2008; Song et al., 2012; Wei et al., 2016). The hierarchical
304 responses to rainfall pulses is commonly recognized in semi-arid ecosystems, which means that small
305 pulses produce minor ecological feedbacks, and greater ones trigger substantial effects (Schwinning and
306 Sala., 2004). These have been confirmed in this study, which clearly showed that rainfall size and month
307 significantly affected the SR (Table 1), and larger rainfall pulses caused greater SR increase (Figs. 5 and 6).
308 In both species and experimental periods, the 5 mm rainfall event did not have a pronounced effect on SR,
309 while significant increases were observed in treatments ≥ 10 mm, suggesting that there might be a threshold
310 rainfall between 5–10 mm for triggering SR responses (Figs. 5 and 6). Considering the aboveground
311 biomass and litter were removed before the experiment, which excluded canopy and litter interceptions, the
312 threshold rainfall should be larger in the natural condition. A threshold rainfall generally exists for
313 promoting the biological response in water-limited ecosystems, which is referred to as ecologically
314 effective rainfall (Schwinning and Sala, 2004). Chen et al. (2008) found that only rainfall events larger than
315 10 mm could significantly increase the SR in the semi-arid grasslands in Inner Mongolia, which is similar
316 to the threshold value observed in this study. While a smaller threshold (3–5 mm) was reported for the same
317 vegetation type also in Inner Mongolia (Hao et al., 2012), this difference could probably be due to their
318 site-specific conditions, such as drier (320–400 mm annual rainfall) than this studied site (540 mm).

319 After comparing the effects of rainfall events in different months, it is suggested that an R_s increase

320 under the same rainfall pulse was relatively larger in August, particularly in *L. davurica* (Fig. 5). Previous
321 studies indicated that rainfall pulses during the dry season with lower antecedent soil water content had
322 greater effects on SR than that during the wet season (Cable et al., 2008; Liu et al., 2017; Morillas et al.,
323 2017). However, this was not the case in our study, where we speculated that the wetter season in this study
324 was still within a relatively dry range, and with larger root respiration and possibly more active microbes
325 (Salazar et al., 2018), the increase in the wet season could exceed that in the dry season. Soil properties
326 (e.g., soil texture and organic matter content) could also affect SR responses after rainfall. In our study, soil
327 texture was unlikely different under the two species since they are growing in the same community.
328 Research showed that soil with more organic matter could release more CO₂ in dry-wet cycles
329 (Harrison-Kirk et al., 2013). The N-fixing *L. davurica* could potentially have higher soil C and N storage
330 below it, like other N-fixing legumes in semi-arid grasslands in the same region (Wu et al., 2017). This
331 organic matter could become available for soil microbes after watering and also the symbiotic
332 nitrogen-fixing bacteria (i.e., rhizobia) activities could be improved after rewetting (Zahran, 1999), with all
333 these subsequently leading to higher SR increments.

334 Soil temperature and soil moisture are two key factors that control SR, and the dependence of SR on
335 these could be altered under different environmental conditions (Almagro et al., 2009). The negative
336 relationship or decoupling between SR and T_s has been reported when the soil water content is below a
337 certain value (Chang et al., 2014). This is also observed in this study in June for both species (Figs. 7 and 8),
338 and it may be due to inhibited soil microbial activity and autotroph respiration under dry conditions
339 (Almagro et al., 2009). The negative relationship between SR and T_s in the dry season could also be
340 expressed by the temperature sensitivity Q_{10} value. Much smaller Q_{10} values were observed in the dry
341 season (0.61 and 0.45 for *B. ischaemum* and *L. davurica* in June, respectively) compared with the wet

342 season (3.22 and 4.31 for *B. ischaemum* and *L. davurica* in August, respectively) (Table 2), which not only
343 indicated that SR was decoupled with T_s in the dry season, but also showed that the temperature
344 dependence recovered in wet conditions. The SR is dominantly determined by S_v when soil moisture is
345 below/above a certain threshold (Almagro et al., 2009; Arredondo et al., 2018; Chang et al., 2014; Xu et al.,
346 2004). After rainfall pulses, S_v solely explained up to 42% and 52% variations of SR in dry and wet seasons,
347 respectively, while T_s only explained up to 25% variability in either period (Table 2). By combining these
348 two factors, the function was only slightly improved (R-square up to 0.47 and 0.60 in dry and wet seasons,
349 respectively) (Table 2). These indicated that rather than T_s , S_v is the leading factor determining SR response
350 after rainfall pulses in this grassland community, which is consistent with results from other types of
351 grassland in semi-arid regions (e.g., Chen et al., 2008; Arredondo et al., 2018). A meta-analysis study also
352 suggested that SR responses following precipitation were mainly driven by soil moisture changes rather
353 than soil temperature across different biomes (Liu et al., 2016).

354 In June, the peak R_s in *B. ischaemum* under all rainfall treatments showed no difference compared to
355 the control treatment, while in *L. davurica* the peak R_s of rainfall treatments were all significantly higher
356 than the control except the 5 mm one (Fig. 6). The R_s increase on the first day after rainfall was also larger
357 in leguminous *L. davurica* in comparison to *B. ischaemum* under all rainfall treatments (Fig. 5). These
358 suggested that the leguminous *L. davurica* responded more substantially to rainfall pulses compared to the
359 herbaceous *B. ischaemum*. Different extents of increase in seasonal soil respiration were also reported from
360 grassland communities with different dominated species on the Loess Plateau, and they argued that the
361 species composition may regulate the dependence of soil respiration on soil temperature and soil moisture
362 and thereby control SR responses after rainfall (Jia et al., 2014). But in this study, we observed similar
363 patterns in the dependence of soil respiration on soil temperature and soil moisture between the two species.

364 Hence, the species-specific response patterns should be likely due to the possible difference in soil organic
365 matter which may be caused by N-fixation in *L. davurica*. Additionally, potential differences in soil
366 microbial community between the two species could also play a role since a recent study has confirmed that
367 legume and grass species could differentially affect soil chemical properties and the soil microbial
368 community (Zhou et al., 2017).

369

370 **4. Conclusions**

371 Soil respiration promptly and significantly increased after pulsed rainfall in a natural grassland
372 community dominated by *B. ischaemum* and *L. davurica* in the hilly-gully region of the Loess Plateau. The
373 magnitude and duration of the increase were positively related to the rainfall size, and rainfall pulses in the
374 relatively wet season produced more pronounced effects than those in the dry season. Such differences may
375 attribute to variations in plant growth, antecedent soil water content, and other biotic and abiotic factors. A
376 threshold rainfall between 5 and 10 mm may exist for triggering a soil respiration increase. Soil
377 temperature was negatively correlated with soil respiration in the dry season yet switched to positive
378 correlation in the wet season, and soil moisture tended to be the dominant controlling factor of soil
379 respiration following rainfall pulses. Plant functional type co-regulated the soil respiration, and N-fixing *L.*
380 *davurica* could release more carbon than *B. ischaemum* after rainfall pulses. We suggest that the
381 species-specific response patterns observed in this study should be considered in evaluating large-scale soil
382 respiration in the background of vegetation restoration along with rainfall pattern changes in semi-arid
383 regions.

384

385

386 **Acknowledgments**

387 This work was financially supported by the Natural Science Foundation of China (41371509 and
388 41771553) and National Key Research and Development Program of China (2016YFC0501703). The authors
389 wish to thank the anonymous reviewer for constructive comments and suggestions.

390

391 **Declarations of interest**

392 None.

393

394 **References**

- 395 Ahlström, A., Raupach, M. R., Schurgers, G., Smith, B., Arneth, A., Jung, M., Reichstein, M., Canadell,
396 J.G., Friedlingstein, P., Jain, A.K., Kato, E., Poulter, B., Sitch, S., Stocker, B. D., Viovy, N., Wang, Y.P.,
397 Wiltshire, A., Zaehle, S., Zeng, N., 2015. The dominant role of semi-arid ecosystems in the trend and
398 variability of the land CO₂ sink. *Science* 348, 895–899.
- 399 Almagro, M., López, J., Querejeta, J. I., Martínez-Mena, M., 2009. Temperature dependence of soil CO₂
400 efflux is strongly modulated by seasonal patterns of moisture availability in a Mediterranean
401 ecosystem. *Soil Biol. Biochem.* 41, 594–605.
- 402 Arredondo, T., Delgado-Balbuena, J., Huber-Sannwald, E., García-Moya, E., Loescher, H.W.,
403 Aguirre-Gutiérrez, C., Rodríguez-Robles, U. (2018). Does precipitation affects soil respiration of
404 tropical semiarid grasslands with different plant cover types? *Agric. Ecosyst. Environ.* 251, 218–225.
- 405 Austin, A. T., Yahdjian, L., Stark, J. M., Belnap, J., Porporato, A., Norton, U., ... & Schaeffer, S. M., 2004.
406 Water pulses and biogeochemical cycles in arid and semiarid ecosystems. *Oecologia* 141, 221–235.
- 407 Birch, H. F. 1958. The effect of soil drying on humus decomposition and nitrogen availability. *Plant Soil.*

408 10, 9–31.

409 Borken, W., Matzner, E., 2009. Reappraisal of drying and wetting effects on C and N mineralization and
410 fluxes in soils. *Global Change Biol.* 15, 808–824.

411 Cable, J.M., Ogle, K., Williams, D.G., Weltzin, J.F., Huxman, T.E., 2008. Soil texture drives responses of
412 soil respiration to precipitation pulses in the Sonoran Desert: implications for climate change.
413 *Ecosystems* 11, 961–979.

414 Chang, C.T., Sabaté, S., Sperlich, D., Poblador, S., Sabater, F., Gracia, C., 2014. Does soil moisture
415 overrule temperature dependence of soil respiration in Mediterranean riparian forests? *Biogeosciences*
416 11, 6173.

417 Chen, Q., Wang, Q., Han, X., Wan, S., Li, L., 2010. Temporal and spatial variability and controls of soil
418 respiration in a temperate steppe in northern China. *Global Biogeochem. Cy.* 24, GB2010.

419 Chen, S., Lin, G., Huang, J., He, M., 2008. Responses of soil respiration to simulated precipitation pulses in
420 semiarid steppe under different grazing regimes. *J. Plant Ecol.* 1, 237–246.

421 Davidson, E., Belk, E., Boone, R.D., 1998. Soil water content and temperature as independent or
422 confounded factors controlling soil respiration in a temperate mixed hardwood forest. *Global Change*
423 *Biol.* 4, 217–227.

424 De Deyn, G.B., Cornelissen, J. H., Bardgett, R.D., 2008. Plant functional traits and soil carbon
425 sequestration in contrasting biomes. *Ecol. Lett.* 11, 516–531.

426 Fang, C., Moncrieff, J. B., 2001. The dependence of soil CO₂ efflux on temperature. *Soil Biol. Biochem.* 33,
427 155–165.

428 Fóti, S., Balogh, J., Herbst, M., Papp, M., Koncz, P., Bartha, S., Zimmermann, Z., Komoly, C., Szabó, G.,
429 Margóczy, K., Acosta, M., Nagy, Z., 2016. Meta-analysis of field scale spatial variability of grassland

430 soil CO₂ efflux: Interaction of biotic and abiotic drivers. *Catena* 143, 78–89.

431 Hao, Y.B., Kang, X.M., Cui, X.Y., Ding, K., Wang, Y.F., Zhou, X.Q., 2012. Verification of a threshold
432 concept of ecologically effective precipitation pulse: From plant individuals to ecosystem. *Ecol.*
433 *Inform.* 12, 23–30.

434 Harrison-Kirk, T., Beare, M.H., Meenken, E.D., Condon, L.M., 2013. Soil organic matter and texture
435 affect responses to dry/wet cycles: Effects on carbon dioxide and nitrous oxide emissions. *Soil Biol.*
436 *Biochem.* 57, 43–55.

437 Jia, X.X., Shao, M.A., Wei, X.R., 2014. Response of soil CO₂ efflux to water addition in temperate
438 semiarid grassland in northern China: the importance of water availability and species composition.
439 *Biol. Fert. Soils* 50, 839–850.

440 Kim, D.G., Vargas, R., Bond-Lamberty, B., Turetsky, M.R., 2012. Effects of soil rewetting and thawing on
441 soil gas fluxes: a review of current literature and suggestions for future research. *Biogeosciences*, 9,
442 2459–2483.

443 Li, H.J., Yan, J.X., Yue, X.F., Wang, M.B., 2008. Significance of soil temperature and moisture for soil
444 respiration in a Chinese mountain area. *Agr. Forest Meteorol.* 148, 490–503.

445 Li, J., Huang, Y., Xu, F., Wu, L., Chen, D., Bai, Y., 2018. Responses of growing-season soil respiration to
446 water and nitrogen addition as affected by grazing intensity. *Funct. Ecol.* 32, 1890–1901.

447 Li, J., Li, Z., Lü, Z., 2016. Analysis of spatiotemporal variations in land use on the Loess Plateau of China
448 during 1986–2010. *Environ. Earth Sci.* 75, 1–12.

449 Li, J., Peng, S., Li, Z., 2017. Detecting and attributing vegetation changes on China's Loess Plateau. *Agr.*
450 *Forest Meteorol.* 247, 260–270.

451 Liu, L., Wang, X., Lajeunesse, M.J., Miao, G., Piao, S., Wan, S., Wu, Y., Wang, Z., Yang, S., Li, P., Deng,

452 M., 2016. A cross-biome synthesis of soil respiration and its determinants under simulated
453 precipitation changes. *Global Change Biol.* 22, 1394–1405.

454 Liu, Z., Zhang, Y., Fa, K., Qin, S., She, W., 2017. Rainfall pulses modify soil carbon emission in a semiarid
455 desert. *Catena* 155, 147–155.

456 Lloyd, J., Taylor, J. A., 1994. On the temperature dependence of soil respiration. *Funct. Ecol.* 315–323.

457 López-Ballesteros, A., Serrano-Ortiz, P., Sánchez-Cañete, E.P., Oyonarte, C., Kowalski, A.S., Pérez-Priego,
458 Ó., Domingo, F., 2016. Enhancement of the net CO₂ release of a semiarid grassland in SE Spain by
459 rain pulses. *J. Geophys. Res. Biogeosci.* 121, 52–66.

460 Miao, C., Sun, Q., Duan, Q., Wang, Y., 2016. Joint analysis of changes in temperature and precipitation on
461 the Loess Plateau during the period 1961–2011. *Clim. Dynam.* 47, 3221–3234.

462 Morillas, L., Roales, J., Portillo-Estrada, M., Gallardo, A., 2017. Wetting-drying cycles influence on soil
463 respiration in two Mediterranean ecosystems. *Eur. J. Soil Sci.* 82, 10–16.

464 Niu, F., Duan, D., Chen, J., Xiong, P., Zhang, H., Wang, Z., Xu, B., 2016. Eco-physiological responses of
465 dominant species to watering in a natural grassland community on the semi-arid Loess Plateau of
466 China. *Front. Plant Sci.* 7, 00663.

467 Noy-Meir, I., 1973. Desert ecosystems: environment and producers. *Annu. Rev. Ecol. Syst.* 4, 25–51.

468 Peng, S., Gang, C., Cao, Y., Chen, Y., 2017. Assessment of climate change trends over the Loess Plateau in
469 China from 1901 to 2100. *Int. J. Climatol.* 10.1002/joc.5331.

470 Raich, J.W., Tufekciogul, A., 2000. Vegetation and soil respiration: correlations and controls.
471 *Biogeochemistry* 48, 71–90.

472 Salazar, A., Sulman, B.N. Dukes, J.S., 2018. Microbial dormancy promotes microbial biomass and
473 respiration across pulses of drying-wetting stress. *Soil Biol. Biochem.* 116: 237-244.

474 Schlesinger, W.H., Andrews, J.A., 2000. Soil respiration and the global carbon cycle. *Biogeochemistry* 48,
475 7–20.

476 Schwinning, S., Sala, O. E., 2004. Hierarchy of responses to resource pulses in arid and semi-arid
477 ecosystems. *Oecologia* 141, 211–220.

478 Shu, J.L., 2014. Precipitation redistribution in natural grassland community and its dominant species
479 responses in loess hilly-gully region. Dissertation of Northwest A&F University (in Chinese).

480 Song, W., Chen, S., Wu, B., Zhu, Y., Zhou, Y., Li, Y., Cao, C., Lu, Q., Lin, G., 2012. Vegetation cover and
481 rain timing co-regulate the responses of soil CO₂ efflux to rain increase in an arid desert ecosystem.
482 *Soil Biol. Biochem.* 49, 114–123.

483 Sponseller, R.A., 2007. Precipitation pulses and soil CO₂ flux in a Sonoran Desert ecosystem *Global*
484 *Change Biol.* 13, 426–436.

485 Thomey, M.L., Collins, S.L., Vargas, R., Johnson, J.E., Brown, R.F., Natvig, D.O., Friggens, M.T., 2011.
486 Effect of precipitation variability on net primary production and soil respiration in a Chihuahuan
487 Desert grassland. *Global Change Biol.* 17, 1505–1515.

488 Unger, S., Máguas, C., Pereira, J.S., David, T.S., Werner, C., 2010. The influence of precipitation pulses on
489 soil respiration-Assessing the “Birch effect” by stable carbon isotopes. *Soil Biol. Biochem.* 42, 1800–
490 1810.

491 van 't Hoff, J. H., 1898. *Lectures on Theoretical and Physical Chemistry*, Edward Arnold.

492 Wang, B., Zha, T.S., Jia, X., Wu, B., Zhang, Y.Q., Qin, S.G., 2014. Soil moisture modifies the response of
493 soil respiration to temperature in a desert shrub ecosystem. *Biogeosciences* 11, 259–268.

494 Wei, X., Zhang, Y., Liu, J., Gao, H., Fan, J., Jia, X., Cheng, J., Shao, M., Zhang, X., 2016. Response of soil
495 CO₂ efflux to precipitation manipulation in a semiarid grassland. *J. Environ. Sci.* 45, 207–214.

496 Wu, G.L, Liu, Y., Tian, F.P., Shi, Z.H., 2017. Legumes functional group promotes soil organic carbon and
497 nitrogen storage by increasing plant diversity. *Land Degrad. Dev.* 28, 1336–1344.

498 Xiong, P., Shu, J., Zhang, H., Jia, Z., Song, J., Palta, J. A., Xu, B., 2017. Small rainfall pulses affected leaf
499 photosynthesis rather than biomass production of dominant species in semiarid grassland community
500 on Loess Plateau of China. *Funct. Plant Biol.* 44, 1229–1242.

501 Xu, B., Xu, W., Huang, J., Shan, L., Li, F., 2011. Biomass production and relative competitiveness of a C₃
502 legume and a C₄ grass co-dominant in the semiarid Loess Plateau of China. *Plant Soil* 347, 25–39.

503 Xu, L., Baldocchi, D. D., Tang, J., 2004. How soil moisture, rain pulses, and growth alter the response of
504 ecosystem respiration to temperature. *Global Biogeochem. Cy.* 18, GB4002.

505 Zahran, H.H., 1999. Rhizobium-legume symbiosis and nitrogen fixation under severe conditions and in an
506 arid climate. *Microbiol. Mol. Biol. Rev.* 63, 968–989

507 Zhang, C., Xue, S., Liu, G.B., 2011. A comparison of soil qualities of different revegetation types in the
508 Loess Plateau, China. *Plant Soil* 347, 163–178.

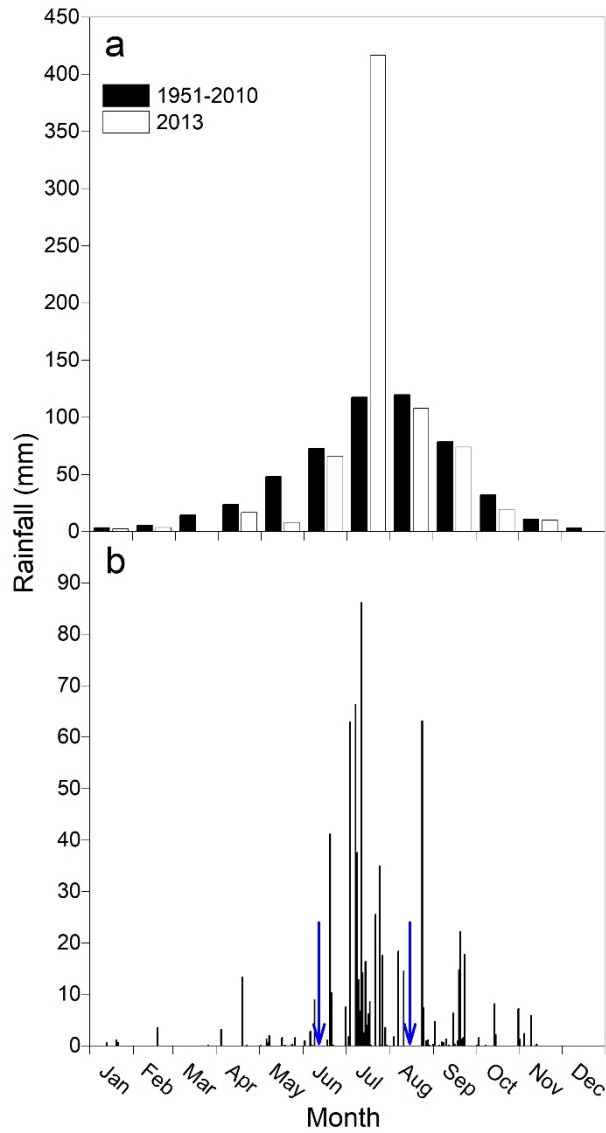
509 Zhang, H., Chen, J., Xiong, P.F., Jia, Z., Wang, Z., Xu, B.C., 2017. Soil respiration response to simulated
510 rainfall pulses in natural grassland communities in Loess hilly-gully region. *Acta Sci. Circumst.* 37,
511 3139–3148. (in Chinese with English abstract)

512 Zhou, Y., Zhu, H., Fu, S., Yao, Q., 2017. Variation in soil microbial community structure associated with
513 different legume species is greater than that associated with different grass species. *Front. Microbiol.* 8,
514 1007.



516

517 **Figure 1.** Photos of the studied grassland community taken from ‘block 1’ in June (a) and August (b) 2013,
 518 and the plot design of the two study blocks established in a homogenous grassland community. The ‘block
 519 1’ (c) was randomly chosen for the experiment in June, and the ‘block 2’ (d) was for the experiment in
 520 August. Numbers inside of squares indicate additional rainfall amounts the plot received during the
 521 respective experimental period besides the ambient.

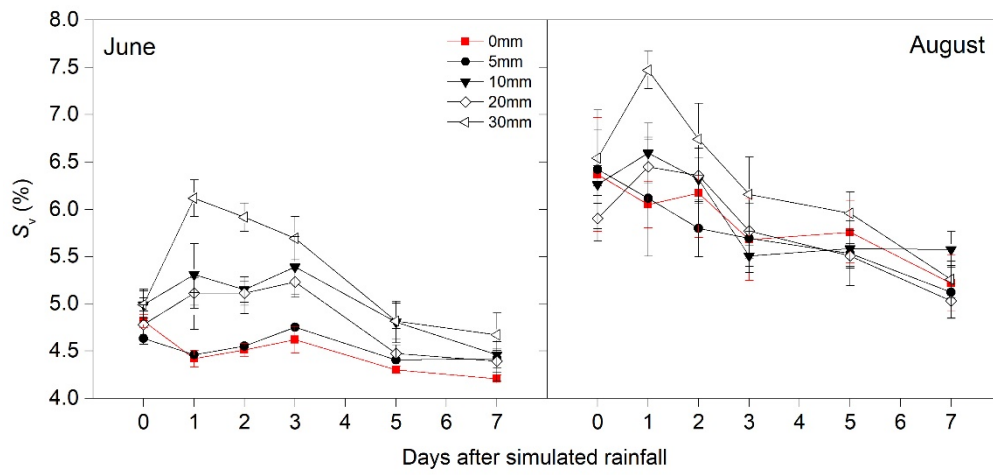


522

523 **Figure 2.** Monthly rainfall in 2013 and average monthly rainfall during 1951–2010 (a) and daily rainfall

524 data in 2013 (b). Blue arrows indicate dates for simulated rainfall experiments (June 12th and August 15th).

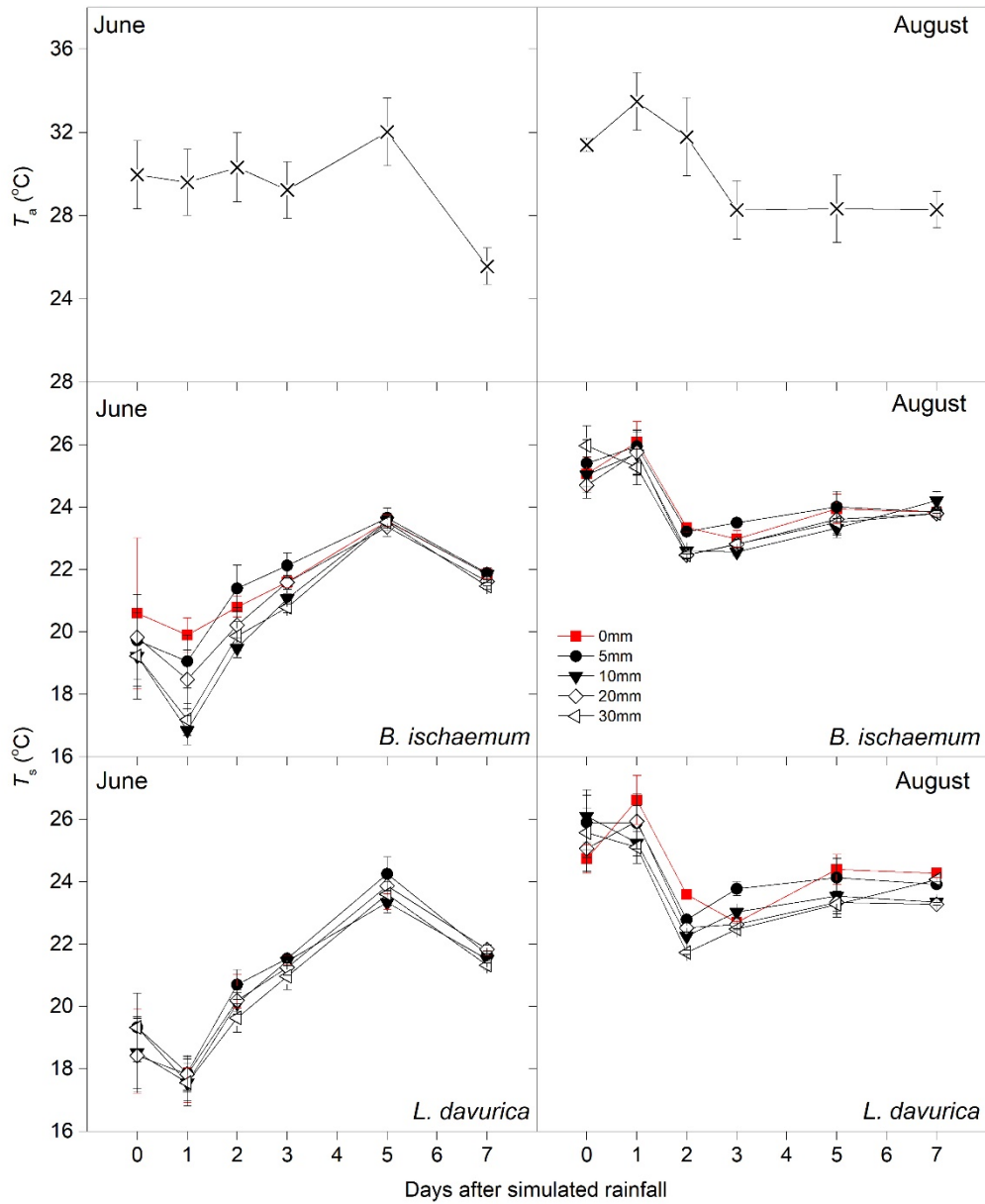
525 Rainfall data were obtained from a meteorological station near the study site (ca. 500 m).



526

527 **Figure 3.** Changes in soil volumetric water content (S_v) after simulated rainfall treatments in June and

528 August 2013. Soil volumetric water content values are averages of 0–20 cm soil depth (mean \pm SE, $n = 3$).



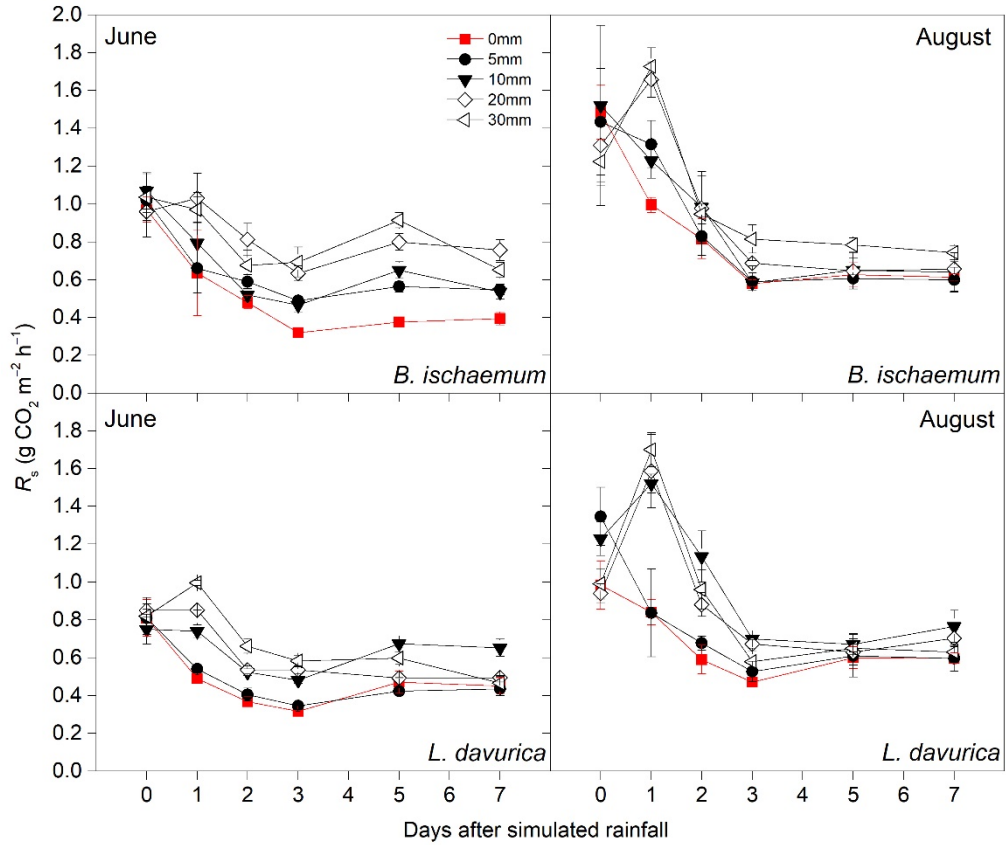
529

530 **Figure 4.** Air temperature (T_a) on different days after simulated rainfall treatments in June and August 2013,

531 and changes in soil temperature (T_s) after simulated rainfall treatments in *B. ischaemum* and *L. davurica* in

532 June and August 2013. Both air temperature and soil temperature data are mean \pm SE ($n = 3$), and soil

533 temperature data are averages of 0–10 cm soil layer.



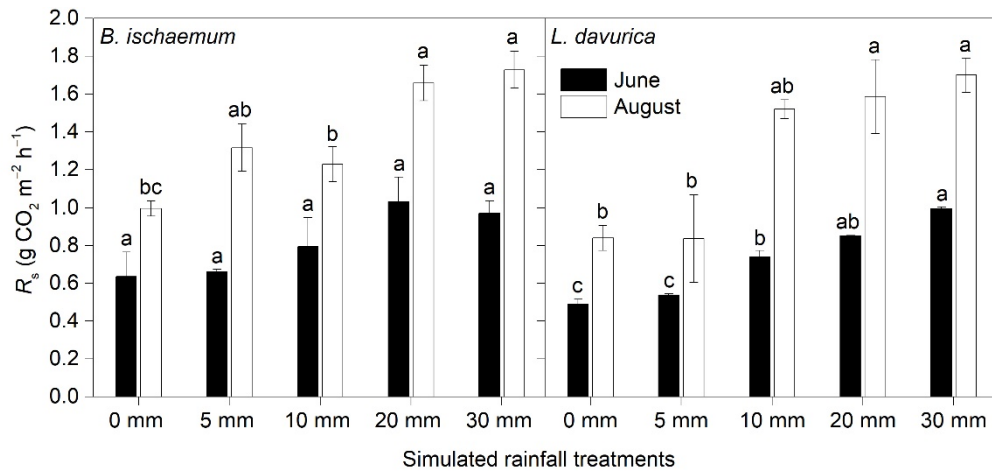
534

535 **Figure 5.** Changes in soil respiration rate (R_s) of *B. ischaemum* and *L. davurica* after simulated rainfall

536 treatments in June and August 2013. Data are instantaneous values (mean \pm SE, $n = 3$) measured between

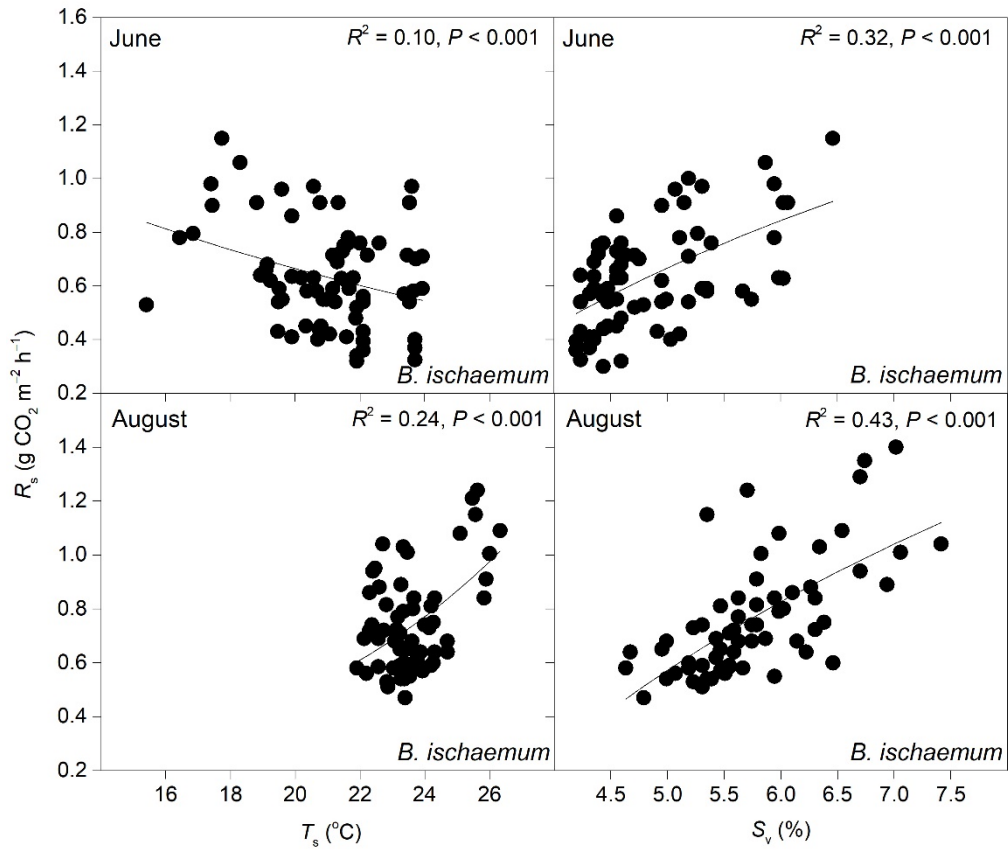
537 9:00–11:00 am on each day.

538



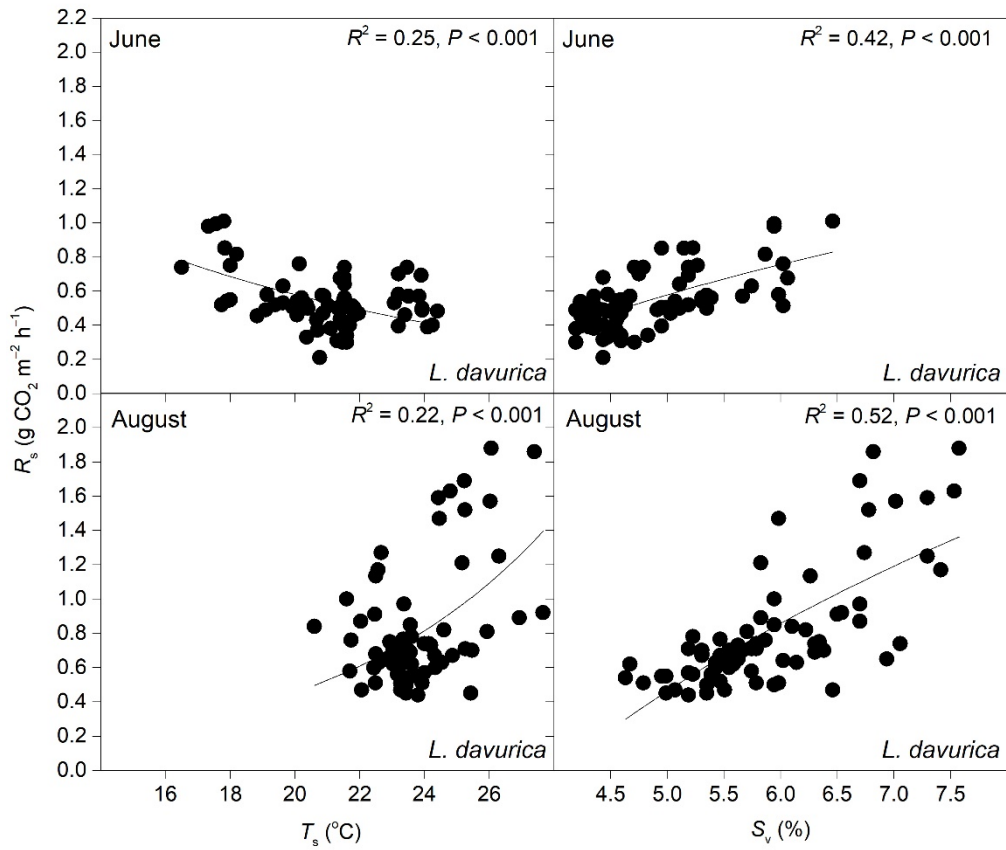
540

541 **Figure 6.** The peak values of soil respiration rate (R_s) of *B. ischaemum* and *L. davurica* after simulated
 542 rainfall treatments in June and August 2013. Data are mean \pm SE ($n = 3$). Different letters above the error
 543 bars indicate significant difference among treatments in the respective month (one-way ANOVA, $P < 0.05$).
 544



546

547 **Figure 7.** Correlations of soil respiration rate (R_s) and soil temperature (T_s) and volumetric soil water548 content (S_v) of *B. ischaemum* in June and August 2013. The exponential function was used for fitting R_s and549 T_s ($R_s = a \times e^{bT_s}$); the logarithmic function for R_s and S_v ($R_s = a \times \ln S_v + b$).



550

551 **Figure 8.** Correlations of soil respiration rate (R_s) and soil temperature (T_s) and volumetric soil water

552 content (S_v) of *L. davurica* in June and August 2013. The exponential function was used for fitting R_s and T_s

553 ($R_s = a \times e^{bT_s}$); the logarithmic function for R_s and S_v ($R_s = a \times \ln S_v + b$).

554 **Tables**

555 **Table 1** Results of two-way/three-way ANOVA for testing the effects of the experimental month, species,
 556 rainfall treatment, and their interactions on soil respiration rate (R_s), soil temperature (T_s), and soil
 557 volumetric water content (S_v) in the investigated grassland community.

	df	R_s		T_s		S_v	
		F	P	F	P	F	P
Month	1	116.42	***	183.35	***	126.90	***
Species	1	10.57	***	0.50	n.s.	-	-
Treatment	4	20.76	***	1.52	n.s.	9.94	***
Month × species	1	0.37	n.s.	0.02	n.s.	-	-
Month × treatment	4	0.33	n.s.	0.02	n.s.	0.98	n.s.
Species × treatment	4	2.94	*	0.06	n.s.	-	-
Month × species × treatment	4	0.75	n.s.	0.40	n.s.	-	-

558 n.s., not significant; *, $P < 0.05$; **, $P < 0.01$; ***, $P < 0.001$. df, degrees of freedom.

559 **Table 2** Regression results of soil respiration rate (R_s) with soil temperature (T_s) and soil volumetric water
 560 content (S_v) in *B. ischaemum* and *L. davurica* in June and August 2013.

R_s vs. T_s	a	b	c	Q_{10}	R^2	P
June						
<i>B. ischaemum</i>	1.81 (0.64)	-0.05 (0.02)		0.61	0.10	<0.001
<i>L. davurica</i>	3.09 (0.97)	-0.08 (0.02)		0.45	0.25	<0.001
August						
<i>B. ischaemum</i>	0.05 (0.03)	0.12 (0.02)		3.22	0.24	<0.001
<i>L. davurica</i>	0.02 (0.02)	0.15 (0.03)		4.31	0.22	<0.001
R_s vs. S_v						
June						
<i>B. ischaemum</i>	0.97 (0.17)	-0.89 (0.27)			0.32	<0.001
<i>L. davurica</i>	0.98 (0.13)	-1.00 (0.21)			0.42	<0.001
August						
<i>B. ischaemum</i>	1.39 (0.20)	-1.67 (0.35)			0.43	<0.001
<i>L. davurica</i>	2.16 (0.25)	-3.02 (0.43)			0.52	<0.001
R_s vs. T_s & S_v						
June						
<i>B. ischaemum</i>	0.17 (0.04)	-0.01 (0.01)	0.14 (0.36)		0.33	<0.001
<i>L. davurica</i>	0.16 (0.03)	-0.02 (0.01)	0.19 (0.26)		0.47	<0.001
August						
<i>B. ischaemum</i>	0.23 (0.03)	0.07 (0.02)	-2.25 (0.43)		0.56	<0.001
<i>L. davurica</i>	0.33 (0.04)	0.07 (0.02)	-2.76 (0.48)		0.60	<0.001

561 R_s vs. T_s , the exponential function $R_s = a \times e^{b \times T_s}$. Temperature sensitivity: $Q_{10} = e^{10b}$. R_s vs. S_v , the
 562 logarithmic function $R_s = a \times \ln(S_v) + b$; R_s vs. T_s & S_v , the binary linear function $R_s = a \times S_v + b \times T_s + c$.
 563 Standard errors of coefficients are given in parentheses.